DEVELOPMENT OF CHITOSAN NANOENCAPSULATED *HOUTTUYNIA CORDATA* THUNB. EXTRACT: EVALUATING THE EFFECT OF EXTRACT CONCENTRATION-LOAD ON MORPHOLOGY, STRUCTURE AND ANTIOXIDANT ACTIVITY

Running Title
HOUTTUYNIA CORDATA THUNB. EXTRACT-LOADED CHITOSAN NANOPARTICLES

NANGWANBIANG KURBAH[1], SHEENA HAORONGBAM[*1], L. ROBINDRO SINGH[*2], YUMNAM SOMI SINGH[3], AND UPASANA DEB[1]

[1] Department of Agribusiness Management and Food Technology, North Eastern Hill University, Tura, Meghalaya - 794002, India
[2] Department of Nanotechnology, North Eastern Hill University, Shillong, Meghalaya - 793022, India
[3] Department of Horticulture, North Eastern Hill University, Tura, Meghalaya - 794002, India

***Corresponding author (s):**
[*1]**SHEENA HAORONGBAM**, email address: sheenahaorongbam@gmail.com,
Orcid ID: https://orcid.org/0009-0000-1976-8720
and
[*2]**L. ROBINDRO SINGH**, email address: lrsingh@nehu.ac.in,
Orcid ID: https://orcid.org/0000-0001-9805-7360

DOI:https://doi.org/10.63001/tbs.2026.v21.i02.S.I(2).pp21336-21367

KEYWORDS

Houttuynia cordata, Chitosan, Nanoparticle, Antioxidant, DPPH, ABTS.

Received on:
31-05-2026
Accepted on:
20-06-2026
Published on:
30-06-2026

Abstract

Houttuynia cordata Thunb. extracted in 80% ethanol (HCE) was loaded in chitosan nanoparticles (HCECS) using sodium tripolyphosphate through the ionic gelation method and the resulting HCECS was evaluated for the effect of extract concentration-load on their morphology, structure and antioxidant activity. The encapsulation efficiency (EE) of HCECS nanoparticles was seen to range from 55.5% to 86.0%, depending on the extract concentration. Particle size ranged from 331 nm to 409 nm, increasing with increase in extract load, while polydispersity index ranged from 0.176 to 0.212, showing a homogenous particle size distribution. Transmission electron microscopy displayed predominantly spherical nanoparticles. FTIR analysis pointed towards the associations between the functional groups of *H. cordata* phytochemicals and the chitosan polymer matrix, confirming successful encapsulation. IC50 values of HCE were 135.77µg/ml and 118.28µg/ml for DPPH and ABTS, respectively. For the HCECS nanoparticle, IC50 value of 299.49µg/ml and 149.90µg/ml at the concentration of 5mg/ml HCE for DPPH and ABTS compared to 1mg/ml HCE, 766.08µg/ml and 159.22µg/ml, respectively were observed. For the nanoparticle formulations, antioxidant activity increased as extract loading increased. The results indicate that there is effect of HCE loading in the formulation of chitosan nanoparticles as well as on the antioxidant activity, which highlights the importance of creating a balance between encapsulation efficiency and antioxidant activity during nanoparticle development for *H. cordata*.

INTRODUCTION

Houttuynia cordata Thunb. is a herb with aromatic and medicinal properties belonging to the Suaruraceae family, and native to Eastern and Southeast Asia (Wu et

al., 2021; Neelam et al., 2025). In India, it is found in the North-Eastern region (Momin et al., 2016; Neelam et al., 2025), with the whole plants of *H. cordata* eaten raw. The plants are used as a medicinal salad to lower blood sugar levels and for blood purification, and the juices from the leaves are used to treat dysentery and cholera (Kumar et al., 2014; Rathi et al., 2013; Hynniewta and Kumar, 2008). *H. cordata* has an ancestry of being used by the Chinese in traditional medicine for cough, bronchitis, and pneumonia (Wu et al., 2021; Pakyntein et al., 2024). Several studies reveal the effects of Houttuynia cordata on Human immunodeficiency virus types-1, Herpes simplex virus, severe acute respiratory syndrome and influenza (Hayashi et al., 1995; Lau et al., 2008; Chen et al., 2011). The plant also has anti-inflammatory, antioxidant, and anticancer properties on account of its several major phenolic, alkaloid, and flavone compounds (Pakyntein et al., 2024). On one hand, the major flavonoid and phenolic compounds are rutin, quercetin, hyperin, isoquercetin, chlorogenic acid, catechin, procyanidin B, hexoside, cepharadione B, aristolactam B, and piperolactam A, act as anticancer, antioxidant, antibiotic and antipyretic antidiabetic agents, additionally, quercetin and chlorogenic acid, a phenolic compounds present in *H. cordata*, impart high and potent antioxidant properties to the plant (Hung et al., 2015; Pradhan et al., 2023; Subhawa et al., 2020; Kumar et al., 2014 and Pakyntein et al., 2024).

With all these multifaceted properties contained in the small herb plant, *H. cordata* has garnered multiple scientific studies from different angles, and is drawing interest in the past few years. A recent work by Neelam et al. (2025) confirmed baseline phytochemical and pharmacognostical analysis of the leaves and roots of *H. cordata* from East Khasi Hills district of Meghalaya in northeast India, and a research for microencapsulation utilizing CS (Chitosan) and CTG (carboxymethyl tamarind gum as

coating material for oil extracted from *H.cordata* has been explored recently for preservation of fresh pork with controlled release of antioxidant and other bioactive compounds creating functional applications (Yang et al., 2025). However, systematic studies for incorporation of different concentrations of extracts from *H. cordata* with bioactive properties and loaded in chitosan at nanoscale level, and thereafter their studies for antioxidant properties remain limited.

In recent years, nano-encapsulation in contrast to microencapsulation, has gained relevance due to its advantages of stability, efficiency, and controlled release (Muhammad, 2022). Nano-encapsulation is used for the protection of bioactive and volatile components from the external environment and has controlled release and targeted delivery systems. It also increases the bioavailability, bio-accumulation, stability, and biodistribution of the encapsulated compounds.

Chitosan is derived from the deacetylation of chitin, a linear polysaccharide from the exoskeleton of crustaceans, insects, and fungi, and has garnered a lot of attention in the medical field because of its cationic nature and varied advantageous properties like pH sensitivity, bio-compatibility, nontoxic, and biodegradability (Ngwuluka et al., 2021). It is a linear cationic polysaccharide of N-acetyl-D-glucosamine and D-glucosamine linked by a β-1-4-glycosidic bond and can be easily worked on and designed for different purposes like nanoparticles, films, and membranes for different applications (Yanat and Schroën, 2021). It was granted by the Food and Drug Administration (FDA) of the USA as GRAS (Generally Recognised as Safe), and can be used as a dietary supplement and wound dressings under the U.S. FDA, 2019a and FDA, 2019b, respectively. It is known for its ability to stimulate the immune system and mucoadhesive capability and has been used as an adjuvant for different vaccine studies, like Anthrax, Hepatitis B and

Schistosoma mansoni (Ghadi et al., 2014). Chitosan has the ability to form hydrogen bonding with phenolic compounds and other functional compounds and interacts electrostatically with them, due to which they are established for effective delivery of the bioactive compounds through targeted and controlled release. This ability is often utilized in nanoencapsulation of the bioactives within chitosan forming bioactive compound-chitosan nanocomplexes, enhancing the stability, dissipation/diffusion, and functional release and expression of the phytochemicals in the targeted environments (Wang et al., 2025). For this application, chitosan is most often utilized by technologies in encapsulation throughout pharmaceutical and food related research. With these considerations, the present study encapsulated phytochemical-rich extracts from *H. cordata*, sourced from Meghalaya in India and was systematically investigated for feasibility in formulating nanoencapsulation of bioactives in chitosan nanoparticles. Further an attempt was made to relate the pure plant extract data with the nanoencapsulated *H. cordata* extract for their antioxidant activity.

MATERIAL AND METHODS

Chemicals

Chitosan (deacetylated 75%) was purchased from Loba Chemie, India. Sodium tripolyphosphate (STTP), Sodium chloride (Nacl), Potassium phosphate monobasic (KH_2PO_4), Potassium chloride (KCl), Sodium phosphate monobasic (Na_2HPO_4) and Potassium persulphate ($K_2S_2O_8$) were purchased from SRL Pvt. Ltd, India. ABTS (2,2-Azinobis (3-ethylbenzothiazoline-6-sulfonic acid) and DPPH (2,2-Diphenyl-1-picrylhydrazyl) were purchased from Sigma-Aldrich, USA.

Plant material

The plants were harvested during the monsoon season from June - September from the wild of East Khasi Hills District, Meghalaya, India, located in the coordinates of N 25° 22' 5.4372", E 91° 45' 13.9752.

Preparation of *Houttuynia cordata* extract (HCE)

The whole plant (leaves, stem, and roots) was washed with water (distilled) and dried at 35°C in the hot air oven. The dried plant was ground into a powder. Thereafter, 100g of powdered plants was soaked in 1 L of 80% ethanol for one week. The soaked sample was filtered with filter paper, and the filtrate was evaporated with a rotary evaporator. The obtained HCE (*Houttuynia cordata* extract) was stored at 4°C for further use (Poolsil et al., 2017).

Preparation of *Houttuynia cordata* extract loaded in chitosan (HCECS) nanoparticles

The *Houttuynia cordata* extract-chitosan (HCECS) nanoparticle were synthesized by the ionic gelation method with slight modification (Koyani and Vazquez-Duhalt, 2016; Chatterjee et al., 2021). Chitosan was dissolved in 1% aqueous acetic acid, and Sodium tripolyphosphate (STPP) was dissolved in water at a ratio of 1:0.5. Three concentrations of *Houttuynia cordata* extract (HCE) were added to the chitosan solution (1, 2.5, and 5 mg./ml) and stirred till it became a homogenous solution. Following this, STPP (Sodium tripolyphosphate) was then added to the homogeneous solution dropwise, with constant stirring for 30 minutes at 800 rpm. The homogeneous solution was then transfer into a 50 ml centrifuge tube and the solution was centrifuged for 15 minutes at 10000 rpm, and the resulting pellet (HCECS) was lyophilise and stored at 4°C for further analysis. Figure 1 shows the flowchart depicting the experimental workflow from synthesis of *H. cordata* extract loaded in chitosan nanoparticles, their physicochemical characterization and analysis of antioxidant activity.

Encapsulation efficiency

The Encapsulation efficiency (EE) was measured by UV-Visible spectroscopy (Agilent Technology, USA) (Liang et al., 2011; Egil et al., 2020). The colloidal suspension was taken in 50 ml centrifuge tube and was centrifuged at 10000 rpm for

10 minutes at 4°. The supernatant was collected and determined for the absorbance at 409 nm. The EE was calculated according the following formula:

$$\text{EE (Entrapment Efficiency) (\%)} = \frac{Total\ amount\ of\ HCE - Free\ amaount\ of\ HCE}{Total\ amount\ of\ HCE} \times 100$$

Characterization

Particle size and Polydispersity Index analysis (PDI)

The average size of the nanoparticles and PDI were analysed using a Zeta-Sizer (Nano ZS90, Malvern analytical), in a folded capillary cell at 25°C room temperature (Costa et al., 2023).

Transmission Electron Microscope (TEM) analysis

The shapes and form of the nanoparticles were recorded using TEM (Transmission Electron Microscope). The nanoparticles were dispersed on a copper grid and was air-dried before analysis (Bin-Jumah et al., 2020).

Fourier Transform Infrared Spectrometer (FTIR) analysis

The synthesized nanoparticles (HCECS) were analysed by FTIR (Fourier Transform Infrared Spectrometer) for their constituents. The nanoparticles were recorded in transmission mode at wavenumbers ranging from 4000 to 400 cm^{-1} (Lazaridou et al., 2020).

Antioxidant activities

The antioxidant activity of the HCE (*Houttuynia cordata* extract) and *Houttuynia cordata*-chitosan (HCECS) nanoparticles was tested using DPPH and ABTS assays, which measure free radical scavenging activity.

DPPH assay

DPPH (2,2-diphenyl-1-picrylhydrazyl) was dissolved in methanol ($0.039 g.L^{-1}$), and different concentrations of HCE and HCECS nanoparticles were added to DPPH in methanol. Both the HCE and HCECS nanoparticle in DPPH solution was incubated for 30 minutes at 37°C. The absorbance was measured at 517 nm using a spectrophotometer along with a blank

(Sayah et al., 2017). Standard ascorbic acid was used. The concentration required to scavenge 50% of the DPPH solution was calculated by the IC_{50} value.

$$\text{DPPH scavenging activity\%} = \frac{Absorbance\ of\ control - Absorbance\ of\ sample}{Absorbance\ of\ control} \times 100$$

ABTS assay

Approximately 7 mM ABTS [2,2'-azino-bis (3-ethylbenzothiazoline-6-sulfonic acid)] and 2.45 mM Potassium persulfate ($K_2S_2O_8$) were dissolved in PBS (phosphate buffered saline) for the production of ABTS cation solution. The cation solution was incubated for 12 to 16 hours in the dark before being used. Concisely different concentrations of HCE were added to the cation solution, followed by 2 minutes of incubation. Then, the HCECS nanoparticles were added to the cation solution and incubated for 60 minutes at 37°C in the dark. The absorbance was measured at 734 nm (Muller and Bohm, 2021; Ghafaripour et al., 2023). Standard ascorbic acid was used, and the concentration required to scavenge 50% of the ABTS cation solution was calculated by the IC_{50} value.

$$\text{ABTS radical scavenging activity\%} = \frac{Absorbnace\ of\ control - Absorbance\ of\ sample}{Absorbance\ of\ control} \times 100$$

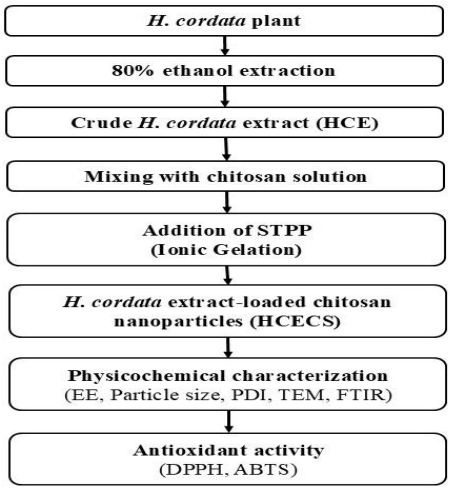

Fig. 1. Experimental workflow – synthesis of *H.cordata* extract loaded in chitosan nanoparticles, their physicochemical characterization and analysis of antioxidant activity

Statistical Analysis

Data are expressed as mean ± Standard deviation (SD). Statistical analysis was performed using one-way ANOVA, with a significance level set at $p<0.05$ was accepted.

RESULTS AND DISCUSSION

Encapsulation efficiency

Encapsulation efficiency of the three different concentrations was analysed by UV-Vis Spectrophotometer (Agilent Technologies, USA). The achieved encapsulation of 1 mg, 2.5 mg, and 5 mg HCECS were 86 ±1.17%, 70.2 ± 1.71% and 55.5 ±2.27%, respectively (significant $p<0.05$ Tukey's post hoc test). The encapsulation of anthocyanin and thyme essential oil-loaded chitosan nanoparticle was reported to be 70% and 98% respectively (Chatterjee et al., 2021; Vafania et al., 2019; Chung et al. (2020) have reported the encapsulation of resveratrol-chitosan nanoparticles between 33 % and 37.1%, while the encapsulation of curcumin, essential oil of thyme, cinnamon and mint loaded chitosan nanoparticle was reported to be 66%, 75.4%, 69.7% and 65.2% respectively. In the current study, the ionic gelation method has been utilised, and the encapsulation efficiency is affected by several factors, such as materials, concentrations and volatility of the compound. Encapsulation of the plant extract by chitosan and the cross-linking properties of sodium tripolyphosphate can stabilise, protect and increase bioavailability of the bioactive compounds (Oakolade et al., 2017; Nouri, 2019). The decrease in encapsulation efficiency with the increase in concentration may be due to the adsorption capacity or chemical saturation of the binding sites in the polymer (CS), which decreases the encapsulation efficiency (Mohammadi et al., 2015), and the increase in CV% denotes that with increase in dose loaded for HCECS, there exhibits greater variability and reduction in stability of the formulation. The results are shown in Table 1.

Table 1: Encapsulation efficiency (EE) of three different concentrations (1, 2.5, and 5 mg) of HCECS nanoparticles

HCECS Dose	EE (%) ± SD	CV%	One-way ANOVA interpretation
1 mg	86.0^{a}±1.17	1.36	F(2,6) = 331.5. p <0.0001
2.5 mg	70.2^{b}±1.71	2.44	
5 mg	55.5^{c}±2.27	4.09	

Legend: HCE – *Houttuynia cordata* extract, HCECS (1mg, 2.5mg and 5mg)– *Houttuynia cordata*-chitosan nanoparticle, CSNP – Unloaded chitosan nanoparticle, CV – coefficient of variation, Data was expressed as mean ± Standard Deviation (SD), n = 3, a, b, c signified different superscripts indicate significant differences (Tukey's post-hoc test, where $p < 0.05$).

Particle size and Polydispersity Index (PDI)

Particle sizes and PDI of the CS, HCECS nanoparticles were analysed by a Zeta-Sizer (Nano ZS90, Malvern Analytical). Particle sizes of the unloaded CS, HCECS (1mg), HCECS (2.5mg), and HCECS (5mg) were 297, 331, 354 and 409 nm, respectively (Table 2 and Fig. 2 A-D). The PDI (Polydispersity Index) measured the particle distribution in a suspension. The PDIs were 0.605, 0.176, 0.181, 0.212 for unloaded CS, HCECS (1mg), HCECS (2.5mg), and HCECS (5mg), respectively (Fig. 2 A-D). PDI value, which is closer to 0, is considered homogeneous, whereas greater than 0.3 is considered heterogeneous suspension. Compared to the results, the PDI of HCECS nanoparticles is a homogenous distribution, which is desirable for synthesising nanoparticles (Gonzales et al., 2021). The reported sizes of chitosan nanoparticles synthesised via the ionic gelation method typically ranged from 100 to 300 nm (Fullagar et al., 2017; Bin-Jumah et al., 2020; Kole et al., 2019; Ahmed et al., 2020; Ge et al., 2018). Ha et al. (2019) and Ghormade et al. (2011) reported that the chitosan nanoparticles were sizes 300 to 750nm and 100 to 500 nm, respectively, on one hand, whereas, Barzegar et al. (2023) have reported that the *Eschium amoenum*-chitosan nanoparticles were 98 and 108 nm, and the particle size of *Aloe*

perryi-chitosan nanoparticles was 168 – 214 nm (Aldeyel et al., 2023). Jiang et al. (2024) reported the sizes of 379 and 360 for unloaded and loaded nanoparticles. The PDI (0.605) of the CS nanoparticles is shown to be homogeneous. The size of the nanoparticles synthesized in the present study was also seen to fall within ranges of 297 to 409 nm, (as can be seen from Fig. 2 A-D), which is similar to previous reports by work on chitosan nanoparticles. The PDI of CSNP is more than 0.3, which shows to be heterogenous.

Table 2: Summary of Zeta Sizer Parameters – particle size and polydispersity index (PDI of samples

Sample	Z-Average (nm)	PDI	Intercept	Peak 1			Peak 2		
				Size (nm)	Intensity (%)	Width (nm)	Size (nm)	Intensity (%)	Width (nm)
CSNP (unloaded CS)	297.1	0.605	0.320	19.05	91.3	3.327	316.1	38.7	97.19
HCECS-1 (1 mg loaded HCECS nanoparticle)	331.4	0.176	0.171	331.5	100.0	93.11	–	–	–
HCECS-2.5 (2.5 mg loaded HCECS nanoparticle	354.1	0.181	0.171	364.5	100.0	102.2	–	–	–
HCECS-5 (5 mg loaded HCECS nanoparticle)	409.1	0.212	0.166	398.7	100.0	81.94	–	–	–

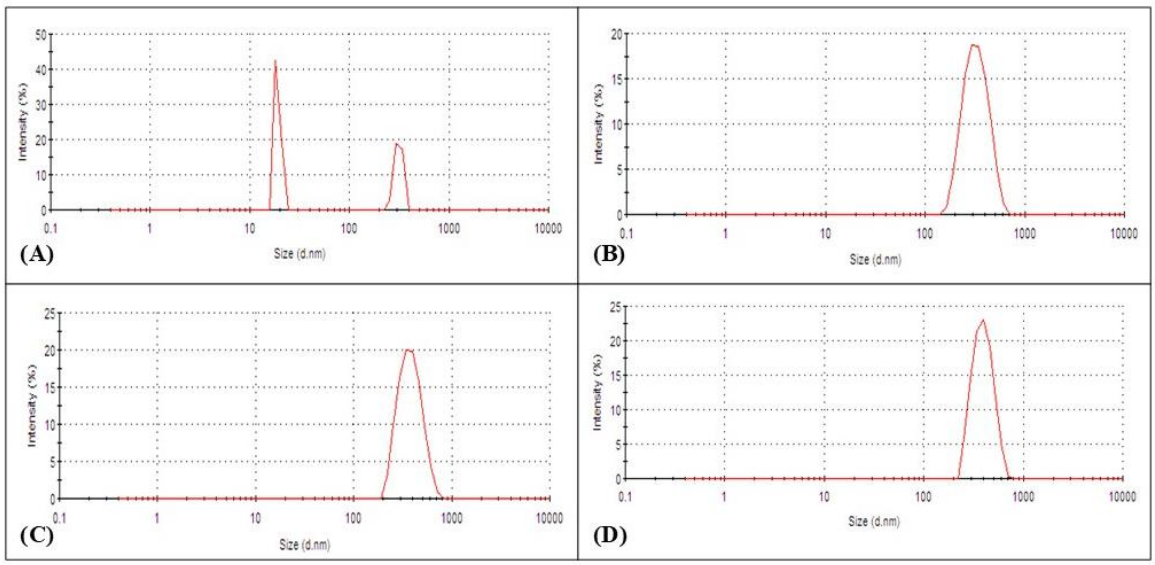

Fig. 2. Particle size distribution profiles of (A) CSNP (unloaded CS), (B) HCECS-1 – 1 mg of extract loaded nanoparticles, (C) HCECS 2.5 – 2.5 mg of extract loaded nanoparticles and , (D) HCECS 5 – 5 mg of extract loaded nanoparticles.

A concentration-dependent trend could be observed, beyond the EE individual values. When the load of HCE for nanoencapsulation was increased from 1 mg to 5 mg (as shown in Table 1 and 2), a gradual decline could be seen in encapsulation efficiency from 86.0% to 55.5%. Such similar decrease in entrapment efficiency has been reported for chitosan-based nanoparticle systems with increase in higher concentrations of load, where the amount of bioactive compound exceeds the effective incorporation capacity of the polymeric matrix (Mohammadi et al., 2015). In the present study, the reduction was not instantaneous, suggesting that the chitosan–STPP network held a significant percentage of the extract even at higher concentration loading levels. However, the lower trends of EE obtained for 2.5 and 5 mg concentration of HCE indicates that further increase of extract concentration was not showing proportional increase in encapsulation. This behaviour may be explained as reflecting competition for binding and entrapment regions among the constituents of the phytochemicals in the extract within the nanoparticle structure, a phenomenon frequently observed when the polymer-to-

cargo ratio becomes less favourable (Lee et al., 2021). Similar observations have been discussed for chitosan nanoparticle formulations, where loading efficiency is governed not only by the quantity of encapsulated material but also by the physicochemical interactions established during nanoparticle formation (Herdiana et al., 2024). Collectively, these findings suggest that maintaining an appropriate extract-to-polymer ratio is critical for achieving efficient encapsulation of HCE in chitosan nanoparticles.

Transmission Electron Microscope (TEM) Analysis

The shapes and form of HCECS nanoparticles were assessed by a Transmission electron microscope (JEOL 200 KV, Japan). The images below (Fig. 3) confirmed the formation of *Houttuynia cordata* nanoparticles (HCECS). The HCECS nanoparticles were well-developed, with a distinct, spherical shape. The spot inside the nanoparticles might be HCE dispersed in STTP-linked in the chitosan polymers complex (Chatterjee et al.,2021; Ge et al., 2018; Manne et al., 2020).

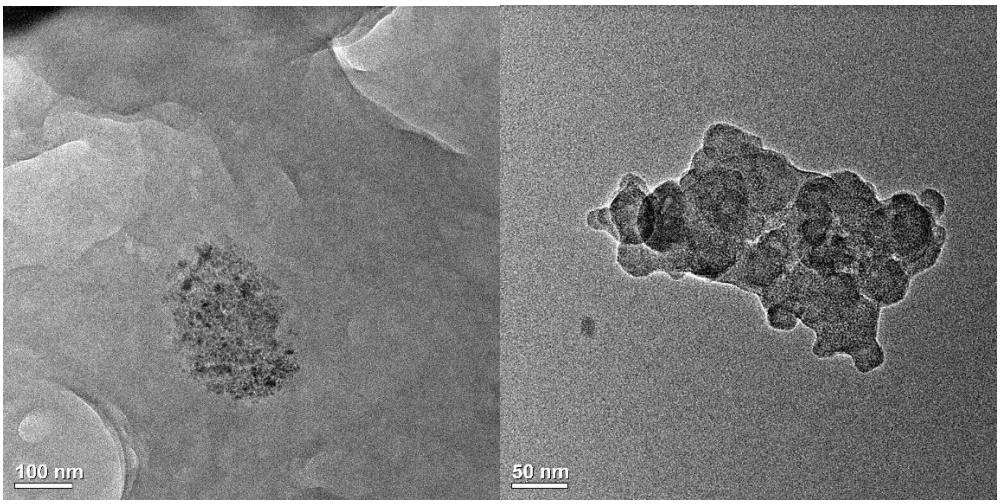

Fig. 3. Transmission electron microscope (TEM) micrography - images of HCECS nanoparticles confirming predominantly spherical nanoparticles and successful encapsulation at nanoscale level

FTIR Analysis

Houttuynia cordata crude extract (HCE) and HCECS nanoparticles were analysed by Bruker Alpha FTIR Spectrometer. The absorption peaks of HCE (Fig. 4) were observed at 3396cm $^{-1}$ (0-H stretching) suggesting the presence of hydroxyl group, the intense peak at 2854 cm^{-1} to 2924 cm^{-1} suggest the C-H (Carbon-Hydrogen) stretching, 1729 cm^{-1} and 1517 cm^{-1} to 1609 cm^{-1} indicate the C=O (Carbonyl, Carbon to Oxygen double bond) stretching of the CHO (aldehyde) or polyphenol, 1055 cm^{-1} to 1453 cm^{-1} suggest to C-O (Carbon-Oxygen) stretching representing the alkoxy group. The FTIR data of the HCE indicate the presence of ketone, polyphenol carbonyl groups (Chen et al., 2023; Kim and Imm, 2018). The absorption peaks of HCECS nanoparticles were observed at 1642 cm^{-1}, 2860-2930 cm $^{-1}$ and 1090-1464 cm $^{-1.}$ The U-shape dip or the broad peak at 3396 cm^{-1} suggests the H-bonding between HCE polyphenols and chitosan amino groups.

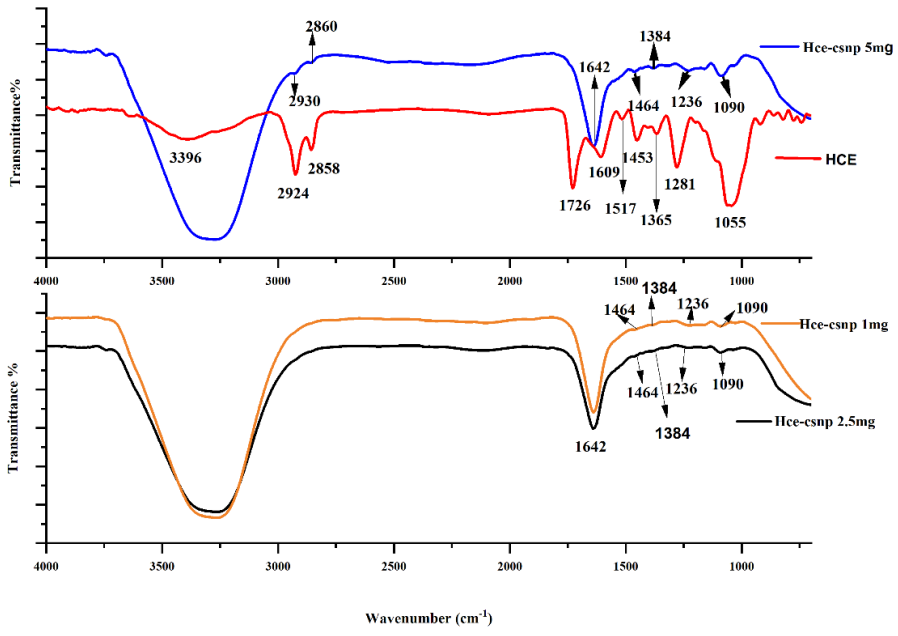

Fig. 4. FTIR spectra of HCE (red), HCECSNP 1mg (orange), 2.5 mg (black), and 5mg (blue)

The intense peak (Fig. 4) observed in all three concentrations (1mg, 2.5mg and 5 mg) at 1642 cm $^{-1}$ represents the amide group, which is on one of the functional groups of CS. The peaks observed from 1090-1464 cm^{-1} showed the overlap of the HCE with CS bands. The extra peaks that we observed in 5mg of HCECS nanoparticles at 2860-2930 cm^{-1} might be due to increased concentration of the HCE, which overlapped with the CS band (Das et al., 2019; Quyen et al., 2018). The FTIR spectra of HCECS nanoparticles displayed observable broadening in the hydroxyl region along with shifts in the characteristic amide bands relative to free HCE. These spectral changes point towards the establishment of intermolecular interactions during nanoparticle formation. Polyphenolic compounds possess numerous hydroxyl groups which can interact with the amino group of chitosan through hydrogen bonding, which is further stabilized by the electrostatic attractions leading to formation of the polymer–bioactive complex (Pattnaik et al., 2022; Wang et al., 2025). In FTIR studies, there have been similar reports for patterns observed in interactions between functional groups in chitosan-based nano delivery systems, which is attributed to the function of hydrogen bonding for associations between phenolic compounds and the chitosan polymer (Zurek and Adamczyk, 2025). The observations in band shifts show that there is molecular interaction between the constituents of HCE and the polymer, though FTIR alone cannot provide evidence for all the intermolecular interactions in the nanoencapsulations. The successful development and retention of *H. cordata* extract in chitosan nanoparticles may be facilitated due to these interactions (Pattnaik et al., 2022; Wang et al., 2025; Zurek and Adamczyk, 2025).

Effect of HCE Concentration Load Citosan Nanoparticle Formulation Behaviour

When EE [Fig. 5 (A)], particle size [Fig. 5 (B)] are observed together alongwith HCE concentration load during nanoparticle formulation, a trend could be observed. The size of the nanoparticle was observed to increase with increase in concentration of HCE-load [Fig. 5 (B)], while a trend of decrease in EE [Fig. 5 (A)] was seen with the increase in extract-load. This

trend may be explained as alteration caused by increased amounts of HCE load on the chitosan matrix organization during the formation of nanoparticles (Lee et al., 2021). Similar observations have been reported, wherein, a balance is to be made between the encapsulated material and the encapsulating polymer for formulation of an efficient nanoparticle with favourable particle characteristics (Lee et al., 2021). Nanoparticles formulated with chitosan polymers have been reported for having limited capacity of load as well as formulation performance affected by the interaction between chitosan matrix and the compounds encapsulated (Herdiana et al., 2024). In the present work, the increase in particle size as well as reduction in encapsulation efficiency (EE) with the increase in loading concentration of HCE suggests that the nanosystem became less efficient at retaining the constituents of HCE as load-concentration increased (Lee et al., 2021; Herdiana et al., 2024).

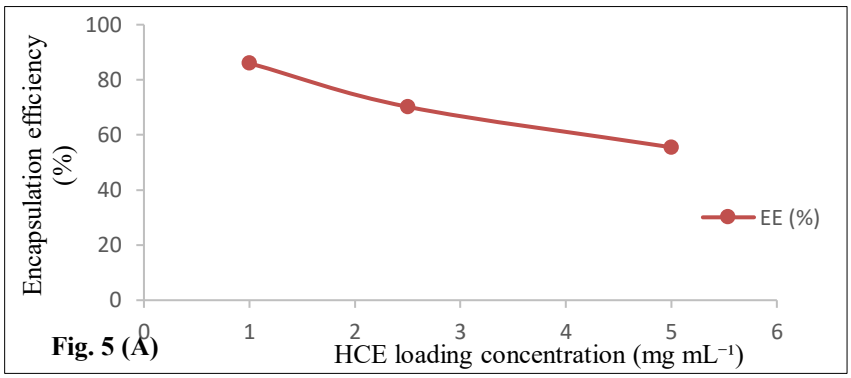

Fig. 5 (A)

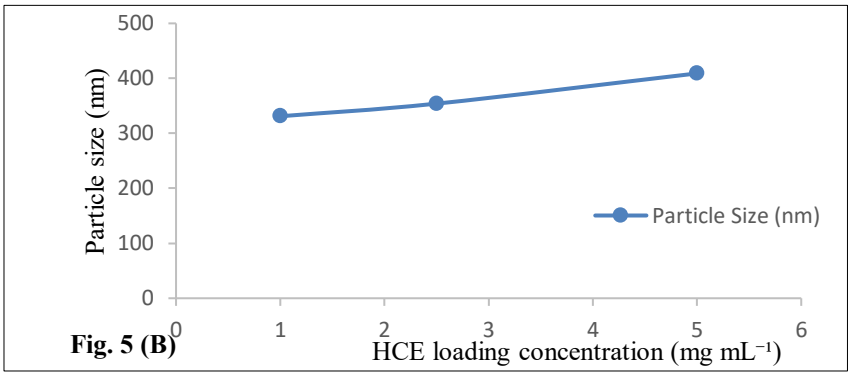

Fig. 5 (B)

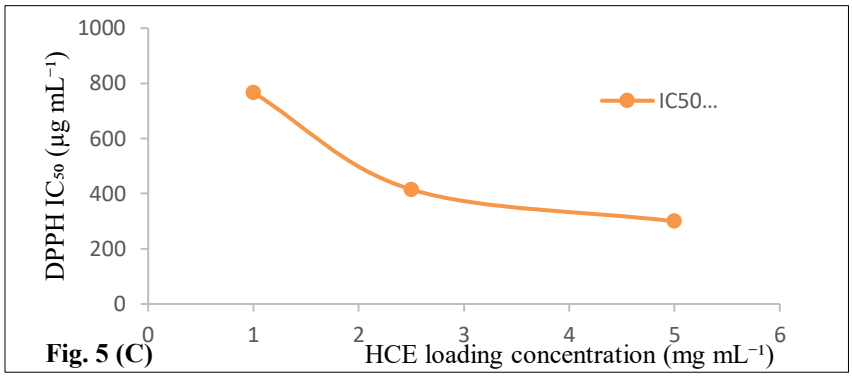

Fig. 5 (C)

Fig. 5. Influence of *Houttuynia cordata* extract loading concentration on formulation characteristics and antioxidant activity of HCECS nanoparticles. (A) Encapsulation efficiency (%); (B) particle size (nm); (C) DPPH IC_{50} (µg mL^{-1}) as affected by increasing HCE loading concentration.

These findings draw focus towards a relationship between HCE load and encapsulation efficiency (EE) in the formulation of the HCECS nanoparticles. Lower HCE concentrations yielded smaller sized nanoparticles with better EE, suggesting more efficient incorporation of bioactive compounds in the HCE. This can be interpreted as, higher HCE loading, which means increase in total amount of HCE associated with the nano formulation, produced larger sized particles and lesser

EE. These trends in formulation behaviour can be utilized in selecting application-specific formulations, since the most effective and efficient nanosystem may not necessarily mean as containing the highest quantity of bioactive material (Herdiana et al., 2024).

In Fig. 5 (A), (B) and Fig. (C), as can be seen, an increase in HCE loading yielded reduced EE [Fig. 5 (A)], while simultaneously increasing particle size [Fig. 5 (B)] and antioxidant activity [Fig. 5 (C)]. Although the efficiency of entrapment declined, the greater amount of incorporated extract appeared sufficient to enhance radical scavenging activity. The results therefore suggest that optimisation of HCECS formulations requires balancing encapsulation performance with the desired functional properties of the final nanoparticle system.

Antioxidant Activity Analysis

Antioxidant activity analysis was performed using a UV-Vis Spectrophotometer (Agilent Technologies, USA). The HCE, HCECS nanoparticles, and CS nanoparticles were analysed against DPPH and ABTS inhibition assays (Table 3). The DPPH scavenging activities (Fig. 6) of HCE, HCECS nanoparticles (5mg, 2.5mg, 1mg) and CSNP with IC_{50} values were found to be 135.77±0.66µg/ml, 299.49±0.59µg/ml, 415.15±1.13µg/ml, 766.08±5.05µg/ml and 2400.02±40.67, respectively, compared to ascorbic acid 75.64±0.03µg/ml ($p < 0.05$). The ABTS scavenging activities (Fig. 7) of HCE, HCECS nanoparticles (5mg, 2.5µg/mg, 1mg) and CSNP with IC_{50} values were 118.28±0.42µg/ml, 149.90±1.17µg/ml, 156.35±0.7µg/ml, 159.22±4.05µg/ml and 1445.29±18.05, respectively ($p < 0.05$), compared to ascorbic acid 74.59 ±1.12µg/ml. Poolsil et al. (2017) have reported the DPPH scavenging activity of HCE with an IC_{50} values of 115.98 µg/ml, Pakyntien et al. (2021) reported that methanol and aqueous extracts have IC_{50} values of 47.94µg/ml and 109.99 µg/ml,

respectively. Kim et al. (2024) and Sakuludomkan et al. (2021) have confirmed that the DPPH and ABTS scavenging activities of HCE with IC_{50} values of 103.3 µg/ml, 37.88 µg/ml and 18.12±0.37µg/ml, 13.83 µg/mL, respectively. The antioxidant activities of HCE were higher as compared to those of the HCECS nanoparticles in both DPPH and ABTS assay analysis. Chatterjee et al. (2021) and Vafania et al. (2019) reported that free anthocyanin and thyme essential oil have higher antioxidant activity than that of the nano-encapsulated NP. This might be because the free phenolic components present in the HCE were able to scavenge the free radical, as compared to the nano-encapsulated HCE, where the phenolic components interact with the polymer (CS) during encapsulation and prevent interaction. The percentage of inhibition for DPPH and ABTS for HCECS (5mg) nanoparticles was observed to be around 80% at 500µg/ml.

Although encapsulation reduced antioxidant activity relative to the free extract, a clear concentration-dependent improvement was observed among the nanoparticle formulations. Increasing HCE loading from 1 mg to 5 mg progressively decreased DPPH IC50 values from 766.08 µg/ml to 299.49 µg/ml and ABTS IC50 values from 159.22 µg/ml to 149.90 µg/ml. The lower the IC_{50} values, greater is the radical scavenging activity of phytochemicals (Gulcin and Alwasel, 2023), which lead to the interpretation that with increase in HCE loading concentrations, the HCECS nanoparticles showed better antioxidant activity in relation to DPPH and ABTS. This increase was accompanied by decline in EE with load-increase, which points towards the suggestion that the antioxidant activity of the extracts was not influenced by the amount of HCE retained in the nanocapsule, but also by the concentration of the HCE loaded in the formulation. Herdiana et al. (2024) have also reported similar findings in nanosystems formed with chitosan polymers, where loading concentration and

EE together influenced the functional behaviour of the final carrier nanosystem. The relationship emphasizes that a highly effective and efficient nanoformulation does not necessarily deliver the maximum amount of bioactive material.

Comparable studies have highlighted that formulation performance in nanosystems is greatly affected by the ratio between the carrier matrix (polymer) and the incorporated bioactive compounds, with optimisation often requiring a balance between loading characteristics and functional outcomes (Lee et al., 2021; Herdiana et al., 2024). Taken together, these findings signifies that nanoformulation optimisation should not rely solely on encapsulation efficiency as a measure of nanoparticle quality. Instead, physicochemical properties and biological functionality should be evaluated collectively to identify formulations that provide the most appropriate balance between structural characteristics and antioxidant performance.

Table 3 IC_{50} Value of ascorbic acid, HCE, HCECS nanoparticles (5,2.5, and 1mg) and CS nanoparticles on DPPH and ABTS assays

Treatments	DPPH activities		ABTS activity	
	IC_{50} (µg/ml)	CV %	IC_{50} (µg/ml)	CV %
Ascorbic acid	77.26^{a}±0.13	0.17	76.91^{a}±0.50	0.65
HCE	135.77^{b}±0.66	0.49	118.28^{b}±0.42	0.36
HCECS (5mg)	299.49^{c}±0.59	0.20	149.90^{e}±1.17	0.78
HCECS (2.5mg)	415.15^{d}±1.13	0.27	156.35^{d}±0.78	0.50
HCECS (1mg)	766.08^{e}±5.05	0.66	159.22^{c}±4.05	2.54
CSNP	2400.02^{f}±40.16	1.67	1445.29^{f}±18.18	1.26
	ANOVA $F(5,12)$, $p<0.05$			

Legend: HCE – *Houttuynia cordata* extract, HCECS (1mg, 2.5mg and 5mg)– *Houttuynia coradata*-chitosan nanoparticle, CSNP – Unloaded chitosan nanoparticle, Data was expressed as mean ± Standard Deviation (SD), n = 3. The results were expressed in IC_{50} (µg/ml)

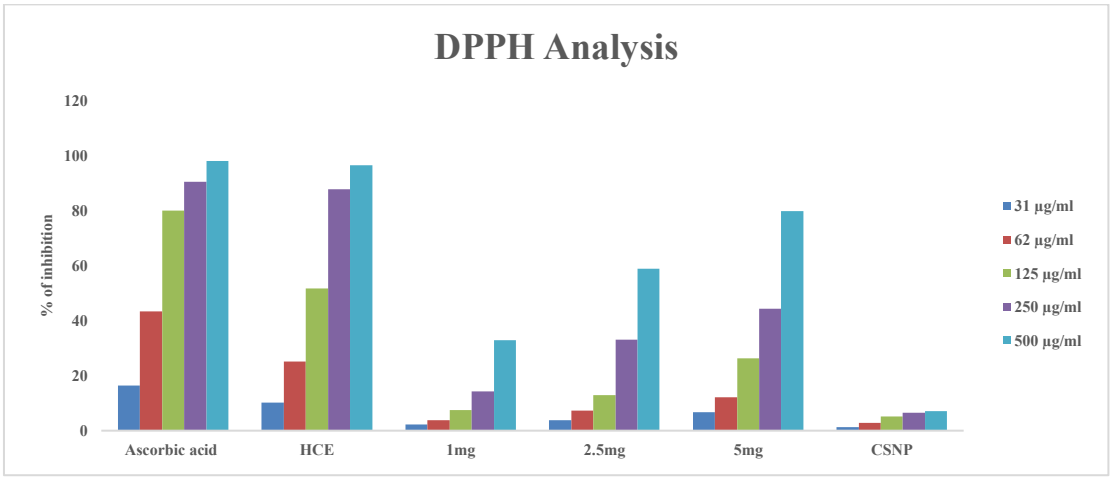

Fig. 6. Percent inhibition of standard, HCE, unloaded CS, and HCECS (1, 2.5, and 5mg) against DPPH

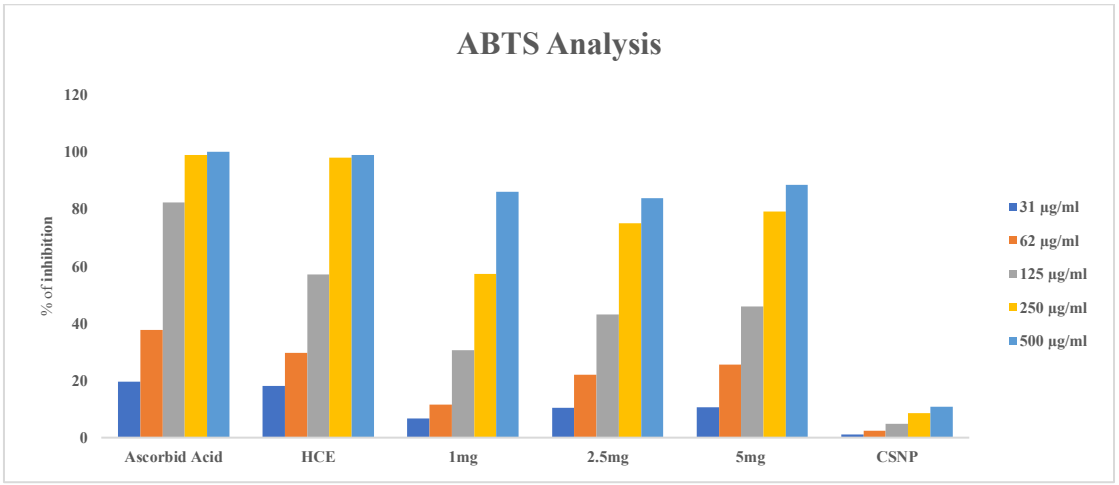

Fig. 7. Percent inhibition of standard, HCE, unloaded CS, and HCECS (1, 2.5, and 5mg) nanoparticles against ABTS

CONCLUSION

The present study illustrated that the HCE-chitosan (HCECS) nanoparticles were successfully synthesised by the ionic gelation method. The HCE-chitosan nanoparticles were characterised by successful encapsulation, and satisfactory encapsulation efficiency. The nanoparticles were seen to be predominantly of spherical shape, and the sizes of the HCECS nanoparticles typically ranged from 200 to 400 nm, with the PDI between 0.1 to 0.6. Changes in extract loading influenced several characteristics of the nanoparticle system. The encapsulation efficiency of the HCECS nanoparticles decreased as the concentrations of loaded HCE extract increased. In contrast, antioxidant activity improved with increasing extract concentration. Nanoencapsulated extract retained antioxidant activity, although the free extract demonstrated stronger radical scavenging properties. Among the formulations studied, the IC_{50} value of the HCECS (5mg) nanoparticles for both DPPH and ABTS assays showed highest activity for radical scavenging. The results suggest that formulations with higher extract loading may provide greater functional activity despite lower encapsulation efficiency. Therefore, selection of an optimum formulation should consider both physicochemical properties and biological performance rather than a single parameter alone. FTIR analysis further corroborate on the interactions developed between the functional groups present in the HCE and the chitosan polymer matrix, validating that the bioactive compounds have successfully integrated in the nanosystem. The results confirm that chitosan polymers can be successfully formulated as a carrier for *H. cordata* extracts. There is a need for further validations into the release studies, antimicrobial, antidiabetic properties, etc., as well as toxicity studies of the nanoencapsulated *H. cordata* extract in order to explore its potential applications in food and nutraceutical systems.

Acknowledgements: The authors gratefully acknowledge the financial assistance provided by the National Fellowship for Higher Studies for Scheduled Tribe (NFST), under the Ministry of Tribal Affairs, Government of India in the form of a scholarship for conducting experiments and analysis.

Conflict of interest: The authors declare no conflict of interest.

Originality of work: The data presented are original and have not been submitted in any journal before.

Approval of statement: The authors approved the final manuscript and are informed of the submission to the Bioscan.

REFERENCES

1. Wu, Z., Deng, X., Hu, Q., Xiao, X., Jiang, J., Ma, X. and Wu, M., 2021. *Houttuynia cordata* Thunb: an ethnopharmacological review. *Front. Pharmacol.,* 12, p.714694. https://doi.org /10.3389/fphar.2021 .714694.
2. Neelam, Patel, O.P. and Soni, G., 2025. Pharmacognostical and Phytochemical Evaluation of *Houttuynia Cordata* Thunb., A Folklore Plant Found in East Khasi Hills, Meghalaya: A Preliminary Study. *J. Chem. Health Risks.,* 15(5), p.610
3. Momin, K.C., Suresh, C.P., Momin, B.C., Singh, Y.S. and Singh, S.K., 2016. An ethno-botanical study of wild plants in Garo Hills region of Meghalaya and their usage. *Int. J. Minor Fruits Med. Aromat. Plants.,* 2016: 47-53
4. Kumar, M., Prasad, S.K. and Hemalatha, S.J.P.R., 2014. A current update on the phytopharmacological aspects of *Houttuynia cordata* Thunb. *Pharmacod. Rev.,* 8(15), p.22. https://doi: 10.4103/0973-7847.125525.
5. Rathi, R.S., Roy, S., Misra, A.K. and Singh, S.K., 2013.

Ethnobotanical notes on *Houttuynia cordata* Thunb. in North-eastern region of India. *Indian J. Nat. Prod. Resour.,* 4(4), pp.432-435.

6. Hynniewta, S.R. and Kumar, Y., 2008. Herbal remedies among the Khasi traditional healers and village folks in Meghalaya. *Indian J. Tradit. Knowl.,* 7(4), pp.581-586.
7. Pakyntein, C.L., Thabah, D., Rai, A.K. and Syiem, D., 2024. Identification of phytoconstituents from *Houttuynia cordata* Thunb. as dipeptidyl peptidase-IV and sodium glucose cotransporter 2 inhibitors guided by molecular docking. *Phytomed. Plus.,* 4(3), p.100590. https://doi.org/ 10.1016/j.phyplu.2024. 100590
8. Hayashi, K., Kamiya, M. and Hayashi, T., 1995. Virucidal effects of the steam distillate from *Houttuynia cordata* and its components on HSV-1, influenza virus, and HIV. *Planta Medica,* 61(03), pp.237-241. https://doi. org/10.1055/s-2006-958063
9. Lau, K.M., Lee, K.M., Koon, C.M., Cheung, C.S.F., Lau, C.P., Ho, H.M., Lee, M.Y.H., Au, S.W.N., Cheng, C.H.K., Bik-San Lau, C. and Tsui, S.K.W., 2008. Immunomodulatory and anti-SARS activities of *Houttuynia cordata. J. Ethnopharmacol.,* 118(1), pp.79-85. https://doi.org /10.1016/j.jep.2008.03. 018
10. Chen, X., Wang, Z., Yang, Z., Wang, J., Xu, Y., Tan, R.X. and Li, E., 2011. *Houttuynia cordata* blocks HSV infection through inhibition of NF-κB activation. *Antivir. Res.,* 92(2), pp.341-345. https://doi.org/ 10.1016/j.antiviral.2011.09.005
11. Hung, P.Y., Ho, B.C., Lee, S.Y., Chang, S.Y., Kao, C.L., Lee, S.S. and Lee, C.N., 2015. *Houttuynia cordata* targets the beginning stage of herpes simplex virus infection. *PloSOne,* 10(2), p.e0115475.

https://doi.org/10.1371/journal.pone.0115475

12. Pradhan, S., Rituparna, S., Dehury, H., Dhall, M. and Singh, Y.D., 2023. Nutritional profile and pharmacological aspect of *Houttuynia cordata* Thunb. and their therapeutic applications. *Pharmacol. Res. - Mod. Chin. Med.*, 9:100311. https://doi.org/10.1016/j.prmcm.2023.100311
13. Subhawa, S., Chewonarin, T. and Banjerdpongchai, R. 2020. The effects of *Houttuynia cordata* Thunb and piper ribesioides wall extracts on breast carcinoma cell proliferation, migration, invasion and apoptosis. *Molecules.*, 25(5), p.1196. https://doi.org/10.3390/molecules25051196
14. Kumar, M., Prasad, S.K., Krishnamurthy, S. and Hemalatha, S. 2014. Antihyperglycemic Activity of *Houttuynia cordata* Thunb. in Streptozotocin-Induced Diabetic Rats. *Adv. Pharmacol. Pharm. Sci.*, 2014(1), p.809438. https://doi:10.1155/ 2014/ 809438
15. Yang, C., Yang, T., Ma, X., He, Y., Liu, M., Hui, T., Li, R., Li, S., Li, C., Hu, L. and Fang, Z. 2025. Microencapsulation with chitosan-embedded *Houttuynia cordata* oil: Integrating antibacterial and antioxidant properties in pork packaging. *Int. J. Biol. Macromol.,* 314, p.144171. https://doi.org/10.1016/j.ijbiomac.2025.144171
16. Muhammad, D.R.A., 2022. Nanoencapsulation: A new way of using herbs and spices in food and its related products. *Rev. Agric. Sci.,* 10, pp.288-303. https://doi.org/10.7831/ras. 10.0_288
17. Ngwuluka, N.C., Abu-Thabit, N.Y., Uwaezuoke, O.J., Erebor, J.O., Ilomuanya, M.O., Mohamed, R.R., Soliman, S.M., Elella, M.H.A. and

Ebrahim, N.A. 2020. Natural polymers in micro-and nanoencapsulation for therapeutic and diagnostic applications: part I: lipids and fabrication techniques. In Nano-and microencapsulation-techniques and applications. *IntechOpen.* https://doi: 10.5772/intech open. 94856

18. Yanat, M. and Schroën, K. 2021. Preparation methods and applications of chitosan nanoparticles; with an outlook toward reinforcement of biodegradable packaging. *React. Funct. Polym.,* 161, p.104849. https://doi.org/10.1016/j.reactfunct polym.2021.104849
19. Ghadi, A., Mahjoub, S., Tabandeh, F. and Talebnia, F. 2014. Synthesis and optimization of chitosan nanoparticles: Potential applications in nanomedicine and biomedical engineering. *Casp. J. Intern. Med.,* 5(3), p.156. https://pubmed.ncbi.nlm.nih.gov/25202443/
20. Wang, J., Chen, J., Jiang, Y., Yang, B. and Wen, L., 2025. Effect of phenolic hydrogen on the formation of chitosan-prenylated flavonoids nanocomplexes. *Food Hydrocoll.,* 168, p.111523. https://doi.org/ 10.1016/j.foodhyd.2025.111523
21. Poolsil, P., Promprom, W. and Talubmook, C. 2017. Anti-hyperglycemic and Anti-hyperlipidemic Effects of Extract from *Houttuynia cordata* Thumb. in Streptozotocin-Induced Diabetic Rats. *Pharmacogn. J.,* 9(3), p.382. https://doi:10.5530/pj.2017.3.65.
22. Koyani, R.D. and Vazquez-Duhalt, R., 2016. Laccase encapsulation in chitosan nanoparticles enhances the protein stability against microbial degradation. *Environ. Sci. Pollut. Res.,* 23(18), pp.18850-18857. https://doi.org/10.1007/s11356-016-7072-8

23. Chatterjee, N.S., Dara, P.K., Perumcherry Raman, S., Vijayan, D.K., Sadasivam, J., Mathew, S., Ravishankar, C.N. and Anandan, R., 2021. Nanoencapsulation in low-molecular-weight chitosan improves in vivo antioxidant potential of black carrot anthocyanin. *J. Sci. Food Agric*., 101(12), pp.5264-5271. https://doi.org/10.1002/jsfa.11175
24. Liang, J., Li, F., Fang, Y., Yang, W., An, X., Zhao, L., Xin, Z., Cao, L. and Hu, Q., 2011. Synthesis, characterization and cytotoxicity studies of chitosan-coated tea polyphenols nanoparticles. *Colloids Surf. B: Biointerfaces*., 82(2), pp.297-301. https://doi.org/10.1016/j.colsurfb.2010.08.045
25. Egil, A.C., Ozdemir, B., Gok, B., Kecel-Gunduz, S. and Budama-Kilinc, Y., 2020. Synthesis, characterization, biological activities and molecular docking of *Epilobium parviflorum* aqueous extract loaded chitosan nanoparticles. *Int. J. Biol. Macromol.,* 161, pp.947-957. https://doi. org/10.1016/j.ijbiomac.2020.06.066
26. Costa, E.M., Silva, S. and Pintado, M., 2023. Chitosan nanoparticles production: optimization of physical parameters, biochemical characterization, and stability upon storage. *Appl. Sci*., 13(3), p.1900. https://doi.org/10.3390/app13031900
27. Bin-Jumah, M., Gilani, S.J., Jahangir, M.A., Zafar, A., Alshehri, S., Yasir, M., Kala, C., Taleuzzaman, M. and Imam, S.S., 2020. Clarithromycin-loaded ocular chitosan nanoparticle: formulation, optimization, characterization, ocular irritation, and antimicrobial activity. *Int. J. Nanomed.,* pp.7861-7875.

https://doi.org/10.2147/IJN.S269004

28. Lazaridou, M., Christodoulou, E., Nerantzaki, M., Kostoglou, M., Lambropoulou, D.A., Katsarou, A., Pantopoulos, K. and Bikiaris, D.N., 2020. Formulation and in-vitro characterization of chitosan-nanoparticles loaded with the iron chelator deferoxamine mesylate (DFO). *Pharmaceutics.*, 12(3), p.238. https://doi.org/10.3390/pharmaceutics12030238
29. Sayah, K., Marmouzi, I., Naceiri Mrabti, H., Cherrah, Y. and Faouzi, M.E.A., 2017. Antioxidant activity and inhibitory potential of *Cistus salviifolius* (L.) and *Cistus monspeliensis* (L.) aerial parts extracts against key enzymes linked to hyperglycemia. *Biomed Res. Int.,* 2017(1), p.2789482. https://doi.org/10.1155/2017/2789482
30. Müller, L., Fröhlich, K. and Böhm, V., 2011. Comparative antioxidant activities of carotenoids measured by ferric reducing antioxidant power (FRAP), ABTS bleaching assay (αTEAC), DPPH assay and peroxyl radical scavenging assay. *Food Chem.,* 129(1), pp.139-148. https://doi.org/10.1016/j.foodchem.2011.04.045
31. Ghafaripour, H., Homayouni Tabrizi, M., Karimi, E. and Barati Naeeni, N., 2023. Lawsone encapsulated polylactic-co-glycolic acid nanoparticles modified with chitosan-folic acid successfully inhibited cell growth and triggered apoptosis in Panc-1 cancer cells. *IET Nanobiotechnol.,* 17(5), pp.425-437. https://doi.org/10.1049/nbt2.12139
32. Vafania, B., Fathi, M. and Soleimanian-Zad, S., 2019. Nanoencapsulation of thyme essential oil in chitosan-gelatin

nanofibers by nozzle-less electrospinning and their application to reduce nitrite in sausages. *Food Bioprod. Process*., 116, pp.240-248. https://doi.org/10.1016/j.fbp .2019.06.001

33. Gulcin, İ. and Alwasel, S. H., 2023. DPPH radical scavenging assay. *Processes*, 11(8), p. 2248. https://doi.org/10.3390/pr11082248
34. Chung, J.H., Lee, J.S. and Lee, H.G., 2020. Resveratrol-loaded chitosan–γ-poly (glutamic acid) nanoparticles: Optimization, solubility, UV stability, and cellular antioxidant activity. C*olloids Surf. B: Biointerfaces.,* 186, p.110702. https://doi.org/10.1016/j.colsurfb.2 019.110702
35. Akolade, J.O., Oloyede, H.O.B. and Onyenekwe, P.C., 2017. Encapsulation in chitosan-based polyelectrolyte complexes enhances antidiabetic activity of curcumin. *J. Funct. Foods.,* 35, pp.584-594. https://doi.org/10.1016/j.jff.2017.06 .023
36. Nouri, A., 2019. Chitosan nano-encapsulation improves the effects of mint, thyme, and cinnamon essential oils in broiler chickens. *Br. Poult. Sci.,* 60(5), pp.530-538. https://doi.org/10.1080 /00071668. 2019.1622078
37. Mohammadi, A., Hashemi, M. and Hosseini, S.M., 2015. Chitosan nanoparticles loaded with *Cinnamomum zeylanicum essential* oil enhance the shelf life of cucumber during cold storage. *Postharvest Biol. Technol.,* 110, pp.203-213. https://doi.org/10.1016/j.postharvbi o.2015.08. 019
38. Gonzales, C.M., Dalmolin, L.F., da Silva, K.A., Slade, N.B.L., Lopez, R.F.V., Moreto, J.A. and Schwarz, K., 2021. New insights of turmeric extract-loaded PLGA nanoparticles:

development, characterization and in vitro evaluation of antioxidant activity. *Plant Foods Hum. Nutr.,* 76(4), pp.507-515. https://doi.org/10.1007/s11130-021-00929-0

39. Fullagar, B., Rao, W., Gilor, C., Xu, F., He, X. and Adin, C.A., 2017. Nano-encapsulation of bilirubin in pluronic F127–chitosan improves uptake in β cells and increases islet viability and function after hypoxic stress. *Cell Transplant.,* 26(10), pp.1703-1715. https://doi.org/10.1177/0963689717735112
40. Kole, Sajal, Syed Shariq Nazir Qadiri, Su-Mi Shin, Wi-Sik Kim, Jehee Lee, and Sung-Ju Jung. Nanoencapsulation of inactivated-viral vaccine using chitosan nanoparticles: Evaluation of its protective efficacy and immune modulatory effects in olive flounder (*Paralichthys olivaceus*) against viral haemorrhagic septicaemia virus (VHSV) infection. *Fish Shellfish Immunol.*, 91 (2019): 136-147. https://doi.org/10.1016/j.fsi.2019.05.017
41. Ahmed, G.H.G., Fernández-González, A. and García, M.E.D., 2020. Nano-encapsulation of grape and apple pomace phenolic extract in chitosan and soy protein via nanoemulsification. *Food Hydrocoll.,* 108, p.105806. https://doi.org/10.1016/j.foodhyd.2020.105806
42. Ge, J., Yue, P., Chi, J., Liang, J. and Gao, X., 2018. Formation and stability of anthocyanins-loaded nanocomplexes prepared with chitosan hydrochloride and carboxymethyl chitosan. *Food Hydrocoll*, 74, pp.23-31. https://doi.org/10.1016/j.foodhyd.2017.07.029

43. Ha, N.M.C., Nguyen, T.H., Wang, S.L. and Nguyen, A.D., 2019. Preparation of NPK nanofertilizer based on chitosan nanoparticles and its effect on biophysical characteristics and growth of coffee in green house. *Res. Chem. Intermed.*, 45(1), p.51. https://doi.org/10.1007 /s11164-018-3630-7

44. Ghormade, V., Deshpande, M.V. and Paknikar, K.M., 2011. Perspectives for nano-biotechnology enabled protection and nutrition of plants. *Biotechnol. Adv.*, 29(6), pp.792-803. https://doi.org/ 10.1016 /j.biotechadv.2011.06.007

45. Barzegar, F., Bohlouli, S., Fakhri, E., Dizaj, S.M., Memar, M.Y. and Sobhanifar, F., 2023. Preparation and Evaluation of Chitosan nanoparticles containing *Iranian eschium amoenum* extract and its antimicrobial effects on common oral microorganisms. *Open Dent. J.*, 17(1). https://doi:10.2174/ 01187 421062712682310301002 48

46. Aldayel, T.S., M. Badran, M., H. Alomrani, A., AlFaris, N.A., Z. Altamimi, J., S. Alqahtani, A., A. Nasr, F., Ghaffar, S. and Orfali, R., 2023. Chitosan-coated solid lipid nanoparticles as an efficient avenue for boosted biological activities of *Aloe perryi*: antioxidant, antibacterial, and anticancer potential. *Molecules.*, 28(8), p.3569. https://doi.org/10.3390/molecules2 8083569

47. Jiang, T., Wang, Y., Yu, Z. and Du, L., 2024. Synthesis, characterization of chitosan/tripolyphosphate nanoparticles loaded with 4-chloro-2-methylphenoxyacetate sodium salt and its herbicidal activity against *Bidens pilosa* L. *Sci. Rep.*, 14(1), p.18754. https://doi.org/10.1038/s41598-024-69438-9

48. Lee, J.S., Oh, H., Kim, S., Lee, J.H., Shin, Y.C. and Choi, W.I., 2021. A novel chitosan nanosponge as a vehicle for transepidermal drug delivery. *Pharmaceutics.,* 13(9), p.1329. https://doi.org/10.3390 /pharmaceutics13091329

49. Herdiana, Y., Febrina, E., Nurhasanah, S., Gozali, D., Elamin, K.M. and Wathoni, N., 2024. Drug loading in chitosan-based nanoparticles. *Pharmaceutics.*, 16(8), p.1043. https://doi.org/10.3390/ pharmaceutics16081043

50. Manne, A.A., Kumar, A., Mangamuri, U. and Podha, S., 2020. *Pterocarpus marsupium* Roxb. heartwood extract synthesized chitosan nanoparticles and its biomedical applications. *J. Genet. Eng. Biotechnol.,* 18(1), p.19. https://doi.org/10.1186/s43141-020-00033-x

51. Chen, M.X., Haider, M.K., Kim, I.S. and Lee, J.S., 2023. Characterization of antioxidant *Houttuynia cordata* extracts loaded polyurethane nanofibers. *Fash. Text.,* 10(1), p.17. https://doi.org/10.1186/ s40691-023-00333-z

52. Kim, J. and Imm, J.Y., 2018. Biosynthesis of silver nanoparticles mediated by *Houttuynia cordata* leaf extract: Characterization and improvement of anti-inflammatory activity. *CYTA - J. Food.,* 16(1), pp.1055-1063. https://doi.org/10.1080/19476337.2018.1527784

53. Das, S., Singh, V.K., Dwivedy, A.K., Chaudhari, A.K., Upadhyay, N., Singh, P., Sharma, S. and Dubey, N.K., 2019. Encapsulation in chitosan-based nanomatrix as an efficient green technology to boost the antimicrobial, antioxidant and in situ efficacy of *Coriandrum sativum*

essential oil. *Int. J. Biol. Macromol.,* 133, pp.294-305. https://doi.org/10.1016/ j. ijbiomac.2019.04.070

54. Quyen, T.T.B., Khanh, N.Q., Khai, H.C., Qui, N.P. and Thien, D.V.H., 2018. Chitosan nanoparticles in combination with *Houttuynia cordata* leaves extract application in preservation of oranges. *Int. J. Sci. Engineer. Sci.,* 2(11), pp.18-22.
55. Pattnaik, A., Pati, S. and Samal, S.K., 2022. Chitosan-polyphenol conjugates for human health. *Life.,* 12(11), p.1768. https://doi.org/10.3390/life12111768
56. Żurek, N. and Adamczyk, G., 2025. Interactions of Polyphenolic Compounds with Gelling Agents: Health-Promoting Properties and Application in Food Systems. *Gels.*, 12(1), p.30. https://doi.org/10.3390/gels12010030
57. Kim, H.J., Mun, J.S., Oh, S.H. and Kim, J.H., 2024. Antioxidant and Antiaging Activity of *Houttuynia cordata* Thunb. Ethyl Acetate Fraction in Caenorhabditis elegans. *Nutrients.,* 16(23), p.4168. https://doi.org/10.3390/nu16234168
58. Sakuludomkan, W., Yeewa, R., Subhawa, S., Khanaree, C., Bonness, A.I. and Chewonarin, T., 2021. Effects of Fermented *Houttuynia cordata* Thunb. on Diabetic Rats Induced by a High-Fat Diet with Streptozotocin and on Insulin Resistance in 3T3-L1 Adipocytes. *J. Nutr. Metab.*, 2021(1), p.6936025. https://doi.org/10.1155/2021/6936025